

# A fundamental study of the effects of compression on the performance of lead accumulator plates

M. Calábek<sup>a,\*</sup>, K. Micka<sup>b</sup>, P. Bača<sup>a</sup>, P. Křivák<sup>a</sup>

<sup>a</sup>Department of Electrotechnology, Technical University of Brno, Údolní 53, 60200 Brno, Czech Republic

<sup>b</sup>J. Heyrovský Institute of Physical Chemistry, Dolejškova 3, 18223 Prague, Czech Republic

## Abstract

Cycling experiments showed that the behavior of compressed test cells is more reproducible with the new separators (Amer-Sil and Daramic) than with the AGM separators used in our previous work; internal shorts did not appear. Optimum mechanical pressure was found to be close to 4 N/cm<sup>2</sup>, at which the cycle life of positive test electrodes exceeded 600 cycles and that of the negatives was more than 800 cycles, both at 100% DOD. Measurements of pressure changes in test cells with lead sheet counter electrodes showed that the volume changes of positive test electrodes follow the expected course, i.e. expansion on discharge and vice versa. The volume increase of the negatives, which may be attributed to the expander, can be prevented or even overcompensated by the applied mechanical pressure. © 2001 Elsevier Science B.V. All rights reserved.

*Keywords:* Lead accumulator; Positive test electrodes; Negative test electrodes; Separators; Compression

## 1. Introduction

During our studies of the effect of mechanical pressure on the performance of lead accumulator electrodes [1], we observed the formation of conducting bridges in the AGM separators, consisting presumably of lead dioxide. This material was found in the AGM separators after cycling experiments by the group of A.F. Hollenkamp [2] (cf. [3]). The formation of conducting bridges was largely eliminated in our work [1] by addition of a thin paper separator with pore size around 0.03 mm. Our experiments showed that the quality of the separator is of crucial importance for proper functioning of lead-acid cells operating under mechanical pressure. Continuation of this research seemed, therefore, worthwhile. Our measuring apparatus enabled us to follow the pressure changes in lead-acid test cells during charging and discharging. Since the results were not in accord with the common concept about volume changes of active masses, we decided to study also this phenomenon in more detail, on positive and negative electrodes separately.

## 2. Experimental

### 2.1. Electrodes and cells

To investigate the pressure effects on the parameters of lead-acid test cells, the test electrode was placed between two counter electrodes in the usual configuration [1]. The electrodes of dimensions 20 mm × 55 mm × 7 mm were prepared by spreading the industrial paste material on to current collectors consisting of 10 insulated parallel ribs [4,5] in the factory AKUMA (Czech Republic). The ribs were taken from grids of the composition Pb Sb 2.19 Sn 0.20 wt.%. Both counter electrodes were of the same size and design as the test electrode. The electrodes were mutually separated by very little compressible separators that were newly developed by DARAMIC Inc. (Germany) and AMER-SIL S.A. (Luxembourg). Their properties are summarized in Table 1. The thicker Daramic separators contacted (from both sides) the active region of the test electrode and copied closely its surface, thus, ensuring uniform pressure load. The Amer-Sil separators, placed between the Daramic separators and the counter electrodes, surpassed the active electrode surface, thus, preventing the formation of electrically conducting bridges. The electrode system was placed in an equipment that produced a defined pressure on the electrode surface. All that was immersed into a large excess of electrolyte of 1.24 g/cm<sup>3</sup> density in a

\* Corresponding author. Tel.: +420-5-43167147;

fax: +420-5-43167280.

E-mail address: calabek@uete.fee.vutbr.cz (M. Calábek).

Table 1

Volume porosity,  $V_p$ , mean pore size, m.p.s., electrical resistivity, e.r., thickness and compression at 8 N/cm<sup>2</sup> in dry state and wetted with electrolyte for two selected separators

Separator	$V_p$ (%)	m.p.s. ( $\mu\text{m}$ )	e.r. ( $\text{m}\Omega \text{cm}^2$ )	Thickness (mm)	% Compression	
					Dry	Wet
Amer-Sil low silica content FC065 profile	80 <sup>a</sup>	4 <sup>a</sup>	75 <sup>a</sup>	0.792	5.7	5.2
Daramic AJS	81 <sup>a</sup>	0.2 <sup>a</sup>	135 <sup>a</sup>	1.49	4.7	3.0

<sup>a</sup> Nominal values; other data were measured in our laboratory.

polypropylene vessel, thermostated at 35°C. The equipment produced a defined pressure on the active electrode surface by means of a thrust screw [5,6]. The pressure was measured by using tensometric sensors connected with a measuring apparatus and a personal computer.

The systems described enabled measurements of the changes of capacity and resistances of the test electrodes. In contrast to the test electrodes, the counter electrodes with excess capacity were only partially utilized.

Somewhat different cells were constructed for measurements of pressure changes during charging and discharging. The aim was to estimate the role of positive as well as negative electrodes in the overall pressure change. To this end, the counter electrodes were replaced by thin lead sheets. The pressure changes were then given by volume changes of the test electrodes. The lead sheets were corroded to some extent during cycling (cf. Planté formation process), but the corrosion was not important during the first 20 cycles, to which the results presented below refer.

## 2.2. Pressure control and cycling regime

In order to follow the pressure effects, six cells with positive and six cells with negative test electrodes were subjected, by a suitable setting of the thrust screw, to sustained pressures of 0, 1, 2, 4, 6 and 8 N/cm<sup>2</sup> (corresponding to 0, 10, 20, 40, 60 and 80 kPa). After several formation cycles, the electrode systems were subjected to a computer-controlled cycling regime. The cells were discharged at a 4 h rate (0.4–0.5 A) to 1.6 V cut-off voltage and then charged for 8 h with a current of 0.4 A (for positive test electrodes) or 0.7 A (for negative ones) with voltage limitation to 2.45 V. Thus, two cycles daily could be carried out. Prior to the start of every cycle, the resistances of active masses ( $R_m$ ) and the interphase (contact) resistances between the current collector and active material ( $R_k$ ) were measured by our method [7,8]. In addition, the values of the scatter criterion ( $K_{rel}$ ) for the contact resistances were calculated [9,10]. Eventually, the pressure settings and the 4 h rate discharge currents were corrected. During cycling, the terminal voltage and the current values were recorded at 1 min intervals for all the cells under test with the aid of a computer and used to calculate the capacity, the charge passed during charging and the state of charge. The 4 h rate discharge current for the subsequent cycle was also calculated.

In order to monitor systems with lead sheets as counter electrodes, eight cells, four with a positive and four with a negative test electrode in the middle, were subjected to pressures of 1, 4, 6 and 8 N/cm<sup>2</sup>. These values were corrected at the start of every discharge. The cells were cycled with an imposed constant current. The cell pressure was recorded at 1 min intervals during charging and discharging (obtained by evaluation of the output voltage of a tensometric sensor, proportional to the pressure).

## 3. Results

### 3.1. Changes of capacity and resistances of test electrodes during cycling

#### 3.1.1. Positive electrodes

The dependences of the capacity,  $C$ , active mass resistance,  $R_m$ , contact resistance between the current collector and the active mass,  $R_k$  and its scatter criterion,  $K_{rel}$ , on the cycle number for positive electrodes under mechanical pressures of 0, 1 and 4 N/cm<sup>2</sup> are shown in Figs. 1–3. Only every 10th point was recorded for better readability. The end of the cycle life was given by the cycle at which the capacity decreased to 66% of its value (indicated by the horizontal dashed line) corresponding to the 10th cycle. The diagrams for 2, 6 and 8 N/cm<sup>2</sup> were similar to those at 4 N/cm<sup>2</sup>. For comparison, the capacities are summarized for all pressure values in Fig. 4 and the active mass resistances in Fig. 5. It can be seen that the capacity, after several formation cycles, shows practically no correlation with the pressure in accord with our previous findings where either AGM [1] or fritted glass separators [9] were used. (A correlation, if any, is masked by the large scatter of experimental points). In contrast to these, however, the capacity is now much more reproducible and rises slowly with the cycle number up to a flat maximum (Fig. 4) except for the electrode operating without pressure, whose capacity passes through a conspicuous maximum and falls down after about 150 cycles. The active mass resistance of this electrode is somewhat higher than that for the other ones and rises steadily after some 150 cycles (Fig. 5). This behavior is probably due to the expansion of the active mass: the rising porosity causes initially a capacity increase but later the interparticle contacts deteriorate considerably, resulting in a capacity drop (compare [1]).

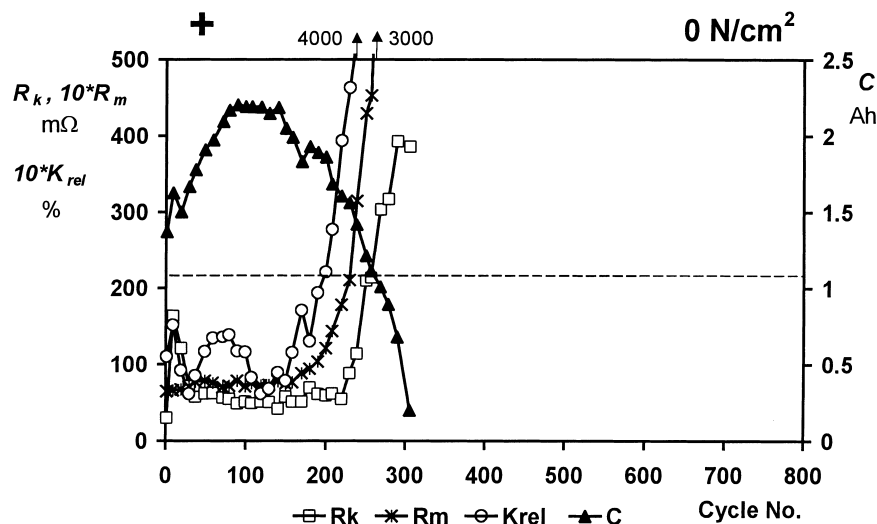


Fig. 1. Evolution of capacity,  $C$ , active mass and interphase resistances,  $R_m$  and  $R_k$  and scatter criterion,  $K_{rel}$ , during cycling. Positive test electrode, cell without compression.

It should be noted that with compressed electrodes, the values of  $R_m$  begin to rise later than the interphase resistance (in contradistinction to non-compressed electrodes [8]), since the interparticle contacts are more or less stabilized.

The interphase resistances show an initial maximum with peak in the region between 5 and 10 cycles; this was also observed in our preceding work using AGM separators [1,6] and in our still earlier work using fritted glass separators [9]; it is apparently related with a slow formation of the active mass/current collector interphase. This maximum, which extends over 20–25 cycles, is well apparent in Fig. 6, summarizing the  $R_k$  characteristics at different pressures. It is accompanied by a similar maximum of the scatter criterion  $K_{rel}$  (compare Figs. 1–3). It seems that the reason

for the slow formation (or equilibration) of the internal electrode structure is due to the fact that the electrode/separator pack is compressed and consequently, the transport of the electrolyte is somewhat hindered. The effect under discussion was not found in our earlier studies with free standing electrodes with lead grids of essentially similar composition [8,9].

In Fig. 7 is shown the dependence of the cycle life on the applied sustained pressure. This resembles the dependence obtained earlier with test cells employing AGM separators combined with microporous paper (ARMORIB) separators [1,11]. It is of practical interest that the optimum mechanical pressure appears to be close to  $4 \text{ N/cm}^2$ . The highest pressure of  $8 \text{ N/cm}^2$  caused (together with corrosion) mechanical damage to the lead grid after about 570 cycles.

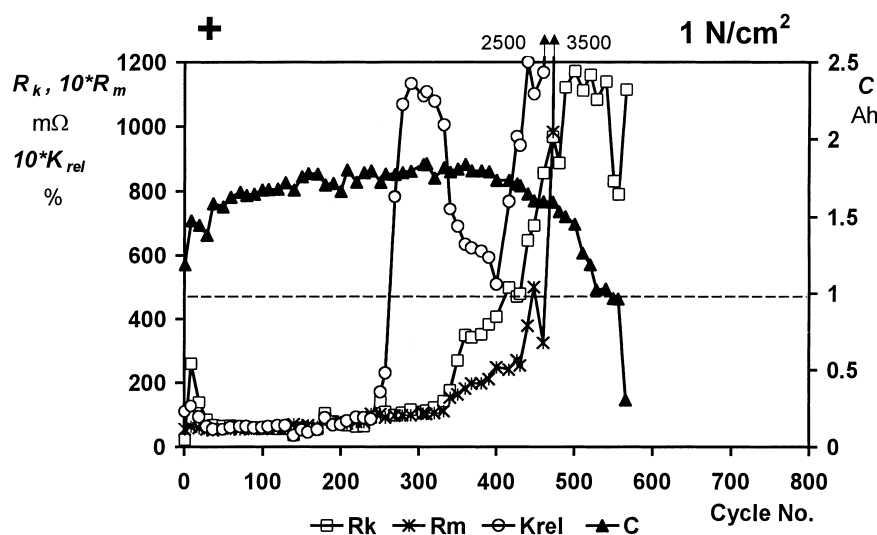


Fig. 2. Evolution of capacity,  $C$ , active mass and interphase resistances,  $R_m$  and  $R_k$  and scatter criterion,  $K_{rel}$ , during cycling. Positive test electrode, cell compressed at  $1 \text{ N/cm}^2$ .

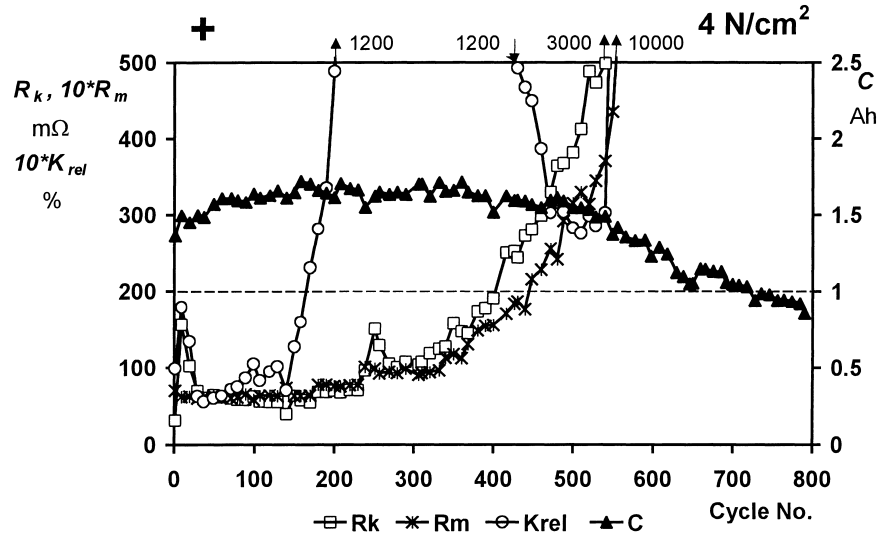


Fig. 3. Evolution of capacity,  $C$ , active mass and interphase resistances,  $R_m$  and  $R_k$  and scatter criterion,  $K_{rel}$ , during cycling. Positive test electrode, cell compressed at  $4 \text{ N/cm}^2$ .

3.1.2. Negative electrodes

Similar cycling dependences for negative electrodes corresponding to pressures of 0, 1 and  $4 \text{ N/cm}^2$  are shown in Figs. 8–10 (the results for 2, 6 and  $8 \text{ N/cm}^2$  were similar to those at  $4 \text{ N/cm}^2$ ). Their capacities are, for comparison, summarized in Fig. 11 and their active mass resistances in Fig. 12. With the cell operating without mechanical pressure, the positive counter electrodes broke down between the 106th and 118th cycles, they were then replaced by new ones, while there was a break in the capacity measurements.

It can be seen from Fig. 11 that the capacity of negative test electrodes, in contrast to the positives, decreases markedly with increasing pressure. It should be noted that a similar phenomenon was observed in our earlier work using fritted glass separators combined with AGM [9] (disregarding the large scatter of experimental points after more than

100 cycles). Also in the present case, where the measurements are more reproducible, the highest and initially moderately increasing capacity was measured without mechanical pressure (a similar trend can be observed at  $1 \text{ N/cm}^2$ ). With the other negative test electrodes, the capacity decreased markedly during the first 100 cycles to reach a steady value. The capacity decrease is more pronounced at higher mechanical pressures. This phenomenon is probably due to a decrease in porosity, caused by the relatively low mechanical strength of the highly porous structure consisting essentially of soft lead dendrites. This view is supported by our studies of pressure changes during cycling (see below).

The active mass resistance,  $R_m$ , in the compressed state is more than an order of magnitude lower than with the positive test electrodes, as found in our previous work [9], and it is practically independent of the cycle number at pressures at

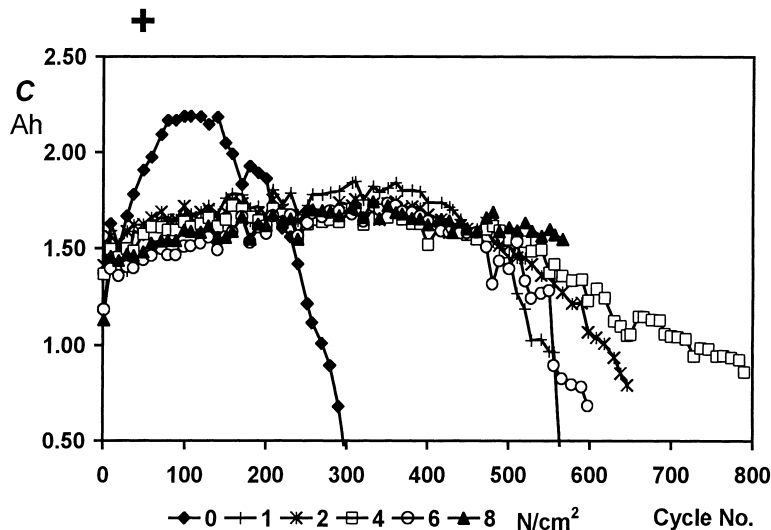


Fig. 4. Evolution of capacity of the positive test electrodes during cycling at pressures 0–8  $\text{N/cm}^2$ .

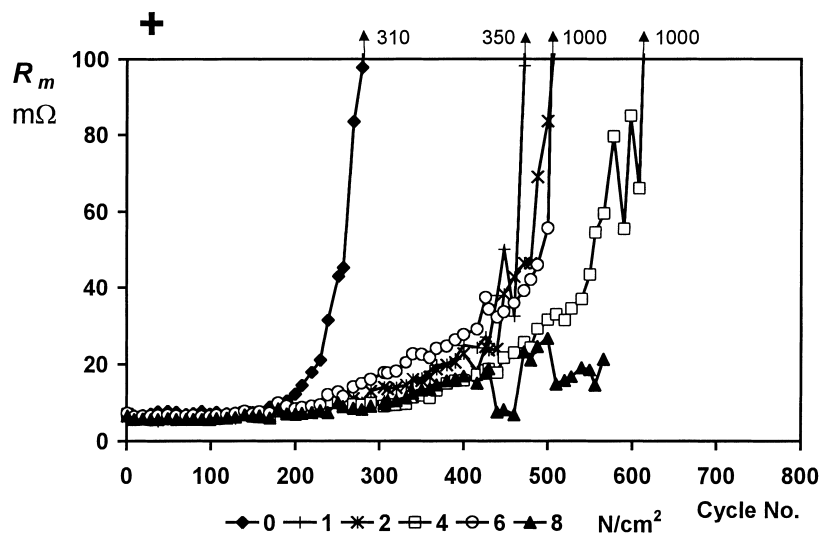


Fig. 5. Evolution of active mass resistance of the positive test electrodes during cycling at pressures 0–8 N/cm<sup>2</sup>.

least 2 N/cm<sup>2</sup> (Fig. 12). (Its values in the discharged state were found to be only a little higher than in the charged state [9]). The interphase resistance,  $R_k$ , for the electrodes compressed at least at 2 N/cm<sup>2</sup> is also very little variable. However, with the electrode operating without pressure, the two resistances show a markedly increasing trend (Fig. 8), indicating an increasing disorder in the active mass and, of course, end of cycle life.

### 3.2. Pressure changes during cycling

The results of measurements on systems with lead sheet counter electrodes (enabling the “net” behavior of a particular electrode to be followed) are shown in Figs. 13–16 for positive electrodes and pressures of 1, 4, 6 and 8 N/cm<sup>2</sup>. The course of the cell voltage,  $U$ , is included for orientation; its dramatic drop at the beginning of discharge to negative

values is caused by the negligible capacity of the counter electrodes. It can be seen that the pressure increases during discharging (Section A) and decreases rapidly during charging (Section B) down to roughly the starting value. This is in accord with the formation and subsequent reduction of the voluminous lead sulphate. Our finding is in support of that of Pavlov and Bashtavelova [12] and other authors (cf. [1,4]), but at variance with the (not very clear) results of Bashtavelova and Winsel [13]. The relative (in percent) pressure increase during discharging is highest at the lowest pressure (about 40%, Fig. 13), as could be expected, and moderate at higher pressures (8–10%, Figs. 14–16).

With negative electrodes, the values of the pressure changes during cycling are appreciably higher than for the positive electrodes (Figs. 17–20). After a small transitory increase at the start of discharge, probably due to lead sulphate formation, there is a steep pressure decrease,

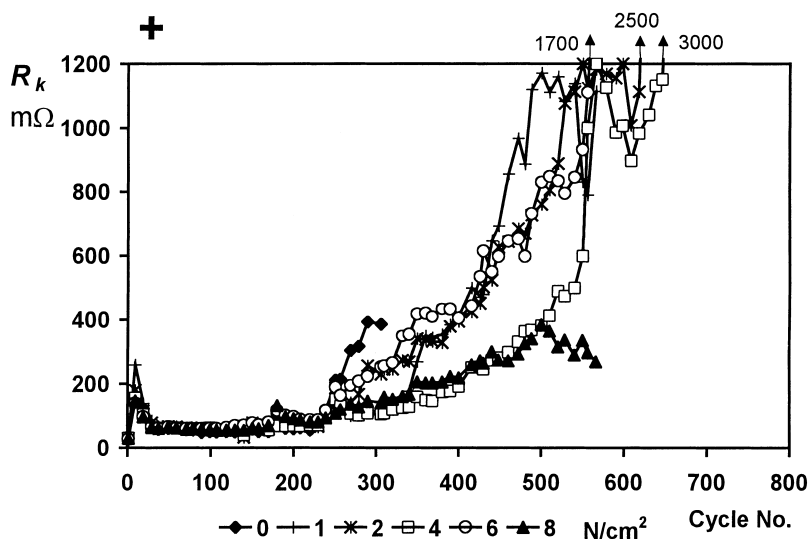


Fig. 6. Evolution of interphase resistance of the positive test electrodes during cycling at pressures 0–8 N/cm<sup>2</sup>.

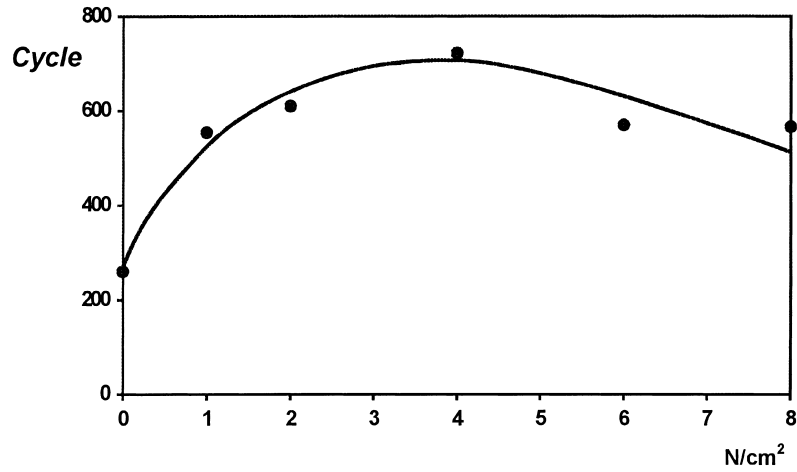


Fig. 7. Dependence of cycle life of positive test electrodes on mechanical pressure. The point at 8 N/cm<sup>2</sup> corresponds to damage of the lead collector ribs.

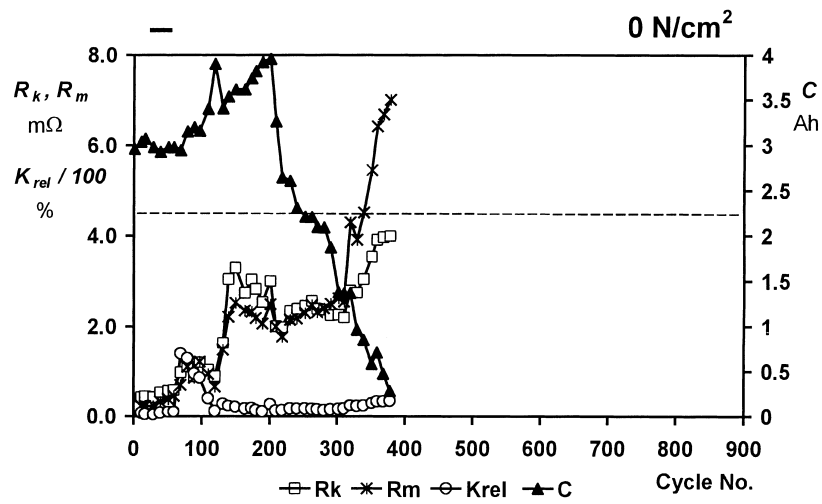


Fig. 8. Evolution of capacity, C, active mass and interphase resistances, R<sub>m</sub> and R<sub>k</sub> and scatter criterion, K<sub>rel</sub>, during cycling. Negative test electrode, cell without compression.

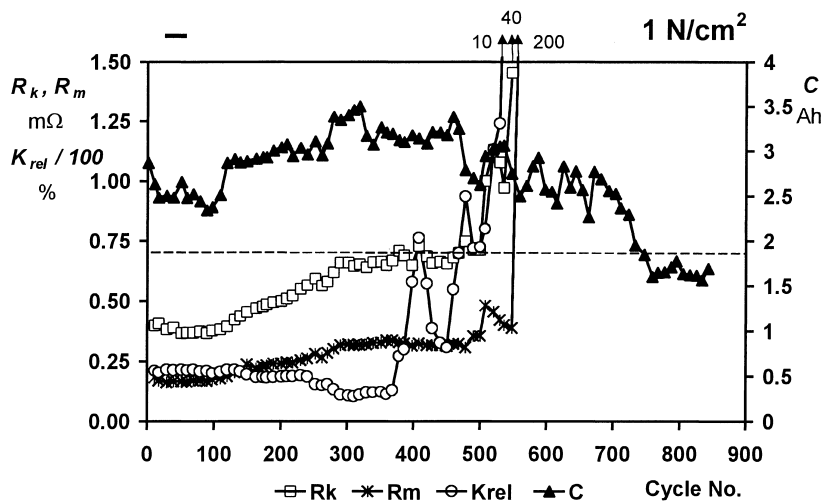


Fig. 9. Evolution of capacity, C, active mass and interphase resistances, R<sub>m</sub> and R<sub>k</sub> and scatter criterion, K<sub>rel</sub>, during cycling. Negative test electrode, cell compressed at 1 N/cm<sup>2</sup>.

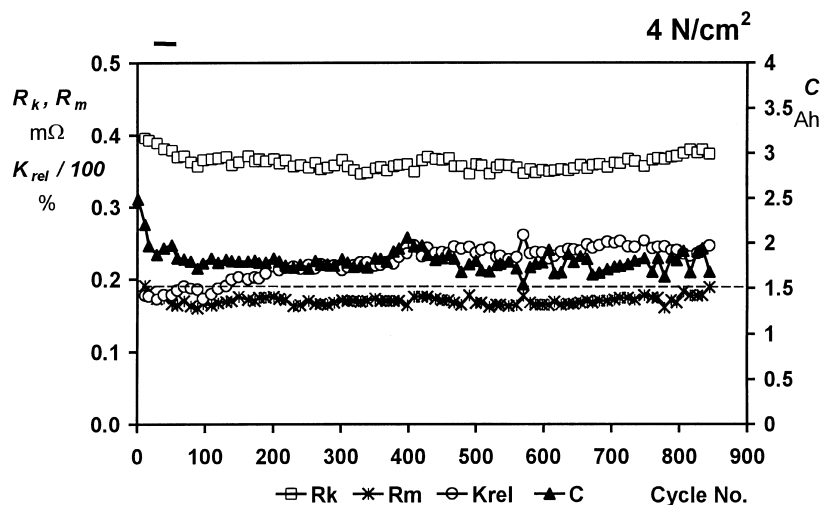


Fig. 10. Evolution of capacity, C, active mass and interphase resistances,  $R_m$  and  $R_k$  and scatter criterion,  $K_{rel}$ , during cycling. Negative test electrode, cell compressed at 4 N/cm<sup>2</sup>.

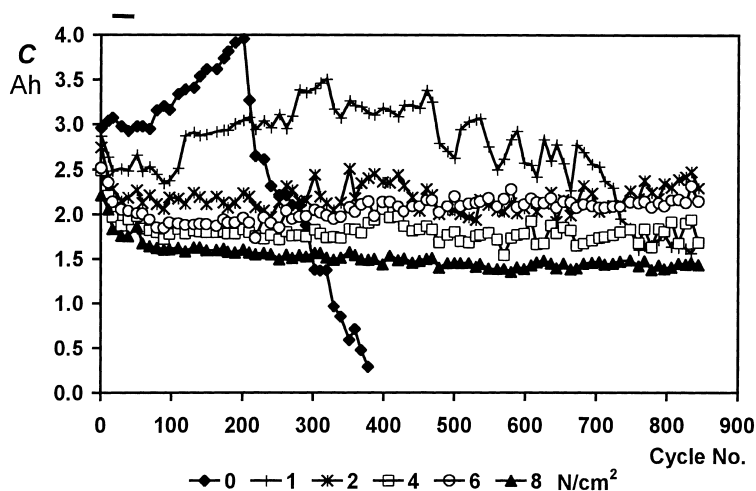


Fig. 11. Evolution of capacity of the negative test electrodes during cycling at pressures 0–8 N/cm<sup>2</sup>.

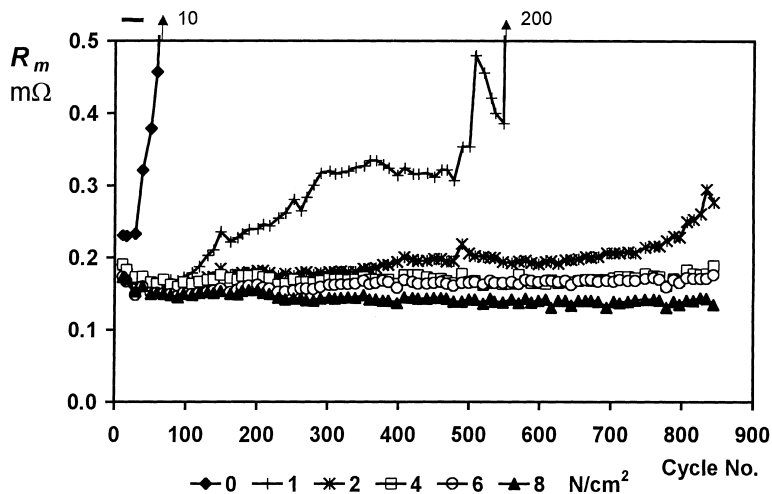


Fig. 12. Evolution of active mass resistance of the negative test electrodes during cycling at pressures 0–8 N/cm<sup>2</sup>.

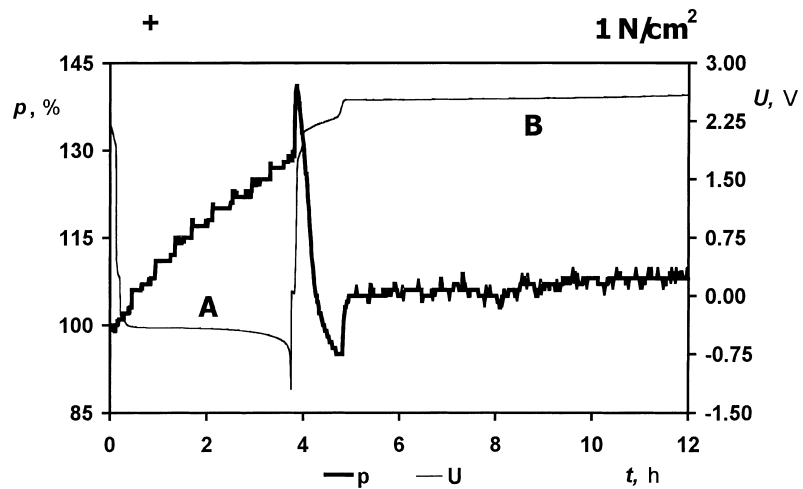


Fig. 13. Time dependence of cell voltage and pressure during discharging and charging. Positive test electrode, lead foil counter electrodes, cell compressed at  $1 \text{ N/cm}^2$ .

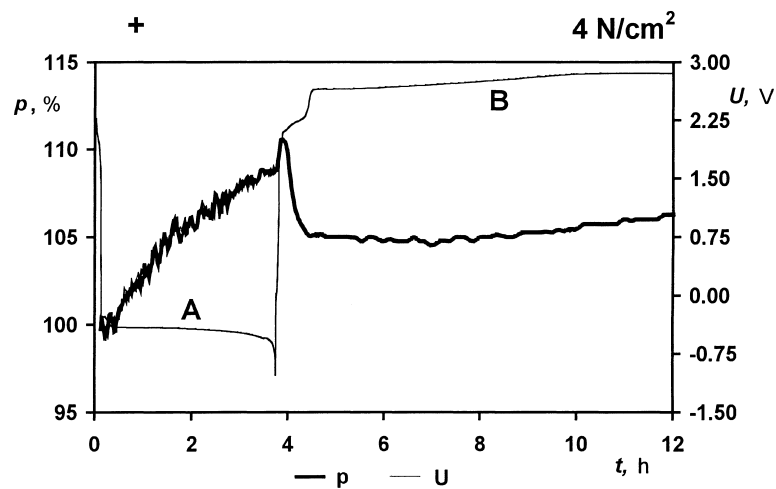


Fig. 14. Time dependence of cell voltage and pressure during discharging and charging. Positive test electrode, lead foil counter electrodes, cell compressed at  $4 \text{ N/cm}^2$ .

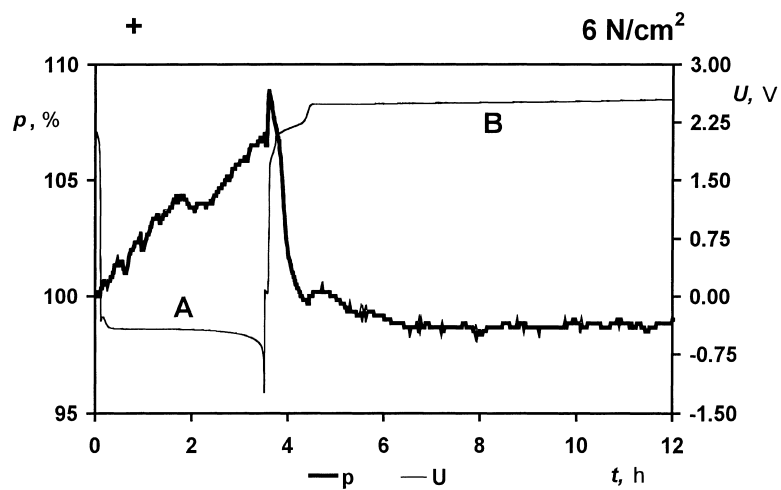


Fig. 15. Time dependence of cell voltage and pressure during discharging and charging. Positive test electrode, lead foil counter electrodes, cell compressed at  $6 \text{ N/cm}^2$ .



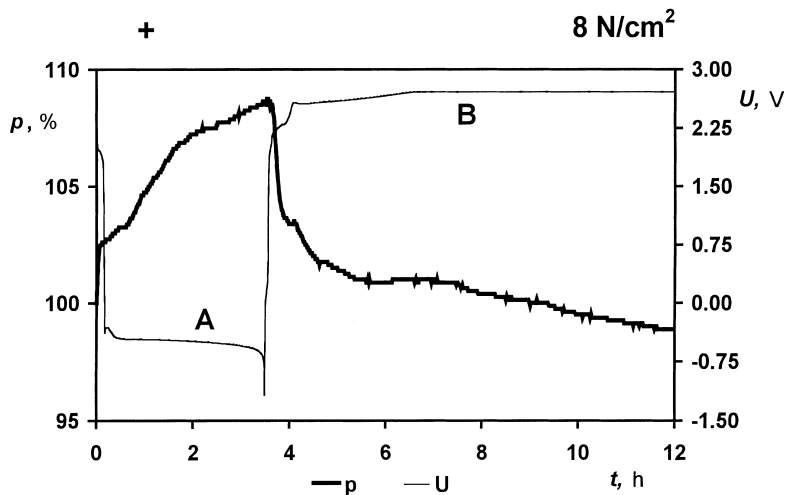


Fig. 16. Time dependence of cell voltage and pressure during discharging and charging. Positive test electrode, lead foil counter electrodes, cell compressed at 8 N/cm<sup>2</sup>.

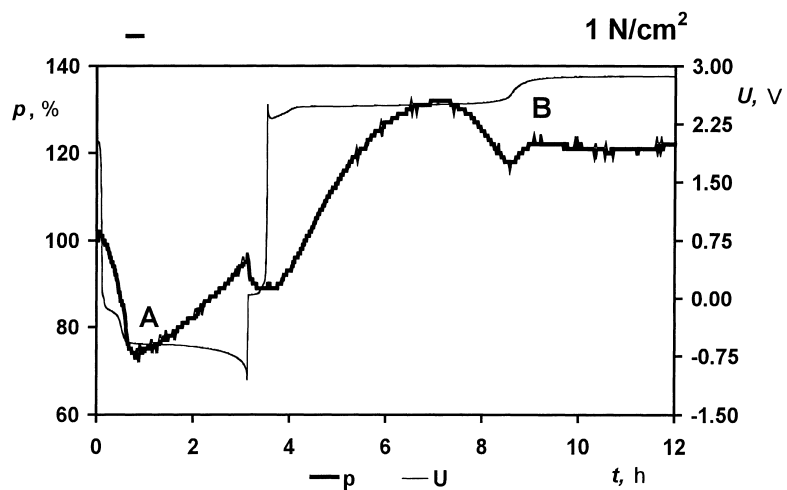


Fig. 17. Time dependence of cell voltage and pressure during discharging and charging. Negative test electrode, lead foil counter electrodes, cell compressed at 1 N/cm<sup>2</sup>.

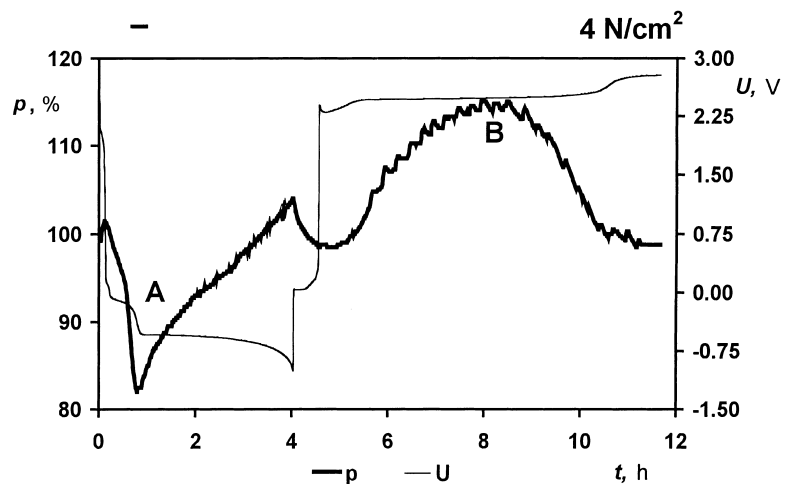


Fig. 18. Time dependence of cell voltage and pressure during discharging and charging. Negative test electrode, lead foil counter electrodes, cell compressed at 4 N/cm<sup>2</sup>.

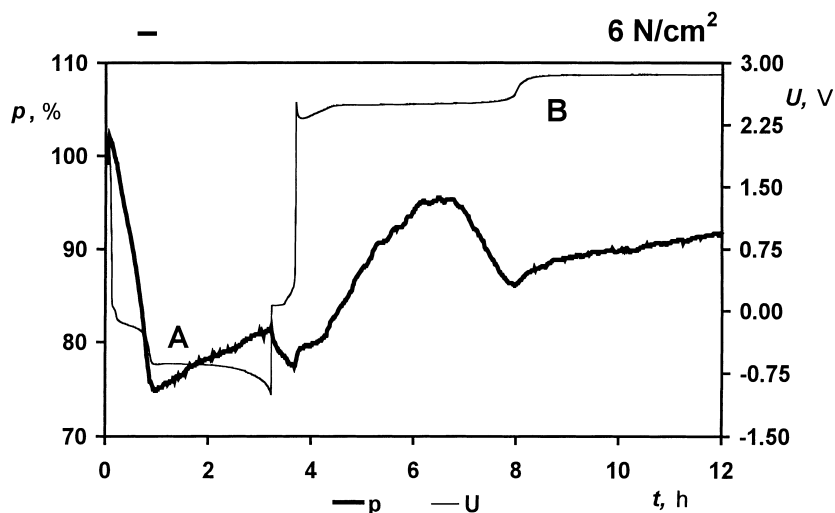


Fig. 19. Time dependence of cell voltage and pressure during discharging and charging. Negative test electrode, lead foil counter electrodes, cell compressed at  $6 \text{ N/cm}^2$ .

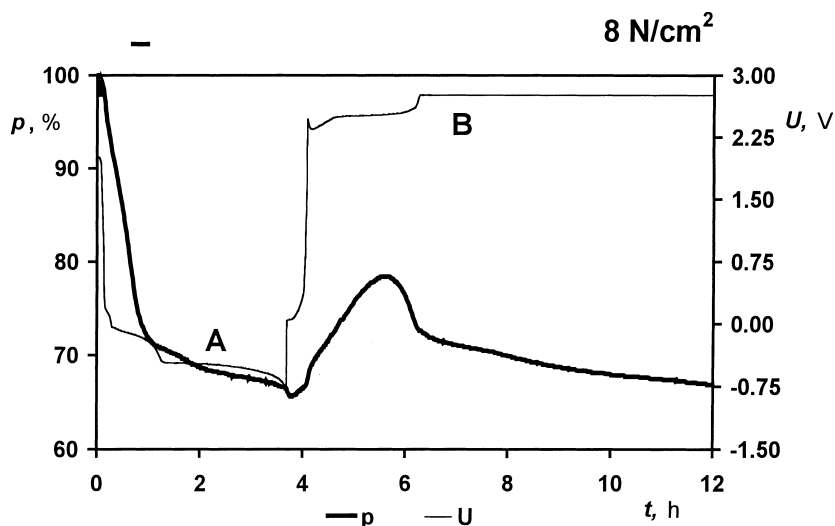


Fig. 20. Time dependence of cell voltage and pressure during discharging and charging. Negative test electrode, lead foil counter electrodes, cell compressed at  $8 \text{ N/cm}^2$ .

probably due to dissolution and softening of the dendritic lead skeleton. This is followed by a pressure increase till the end of discharge (Figs. 17–19), which may be ascribed to the voluminous lead sulphate. However, if the applied pressure is too high, the pressure increase does not take place (Fig. 20). During charging (Section B), the pressure passes through a minimum, presumably due to reduction of  $\text{PbSO}_4$ , followed by a maximum that may be ascribed to the effect of the expander.

The final pressure value is indicative of the stability of the negative electrodes. It can be seen from Figs. 17–20 that at an applied pressure of  $1 \text{ N/cm}^2$  the electrode has a tendency to expand after one cycle, at  $4 \text{ N/cm}^2$  it preserves its volume and at still higher pressures it contracts. In accordance with Fig. 17, Pavlov and Ignatova [14] found a volume increase of non-compressed negative plates on discharge, stating that

the results depend on the expander used. From the practical point of view, it is noteworthy that there exists a pressure value (close to  $4 \text{ N/cm}^2$ ) at which the volume changes of the negative electrodes are suppressed and thus their capacity preserved.

Owing to the rather high porosity of the lead “sponge” skeleton, the electrode can absorb most of the lead sulfate in its pores. The pressure drop during discharge suggests a drop in the mechanical strength of the porous lead skeleton with its resulting slight compression. This may be related with the fact that the discharge capacity of the negative electrodes decreases unexpectedly with increasing pressure (Fig. 11). It is noteworthy that this anomaly was not observed in our preceding work [1] where soft, easily compressible AGM separators were used (allowing the volume changes of the lead electrodes to be well accommodated) and where the

measurement results corresponded to combined changes in thickness of both positive and negative electrodes.

### Acknowledgements

The authors are indebted to AKUMA, Mlada Boleslav, Czech Republic, for providing pasting facilities, K. McGregor and A.F. Hollenkamp (CSIRO, Port Melbourne) for valuable discussions and Mr. Frantisek Korinek and Mrs. Jaroslava Hlavsová for careful technical assistance. Samples of separators were kindly furnished by Werner Böhnstedt (DARAMIC, Inc., Germany) and A.L. de Ferreira (AMERSIL S.A., Luxembourg). This work was supported by the Advanced Lead-Acid Battery Consortium (Project No. B-001.1) a program of the International Lead Zinc Research Organization and by the Grant Agency of the Czech Republic (Grant No. 102/98/1170).

### References

- [1] M. Calábek, K. Micka, P. Bača, P. Křivák, L. Šácha, ALABC Project No. B-001.1, Annual report, January–December, 1998. Technical University Brno, 602 00 Brno, Czech Republic, January 1999, p. 38.
- [2] A.F. Hollenkamp, K. McGregor, M. Barber, J.A. Hamilton, T.D. Huynh, H. Ozgun, C.G. Phyland, A.J. Urban, D.G. Vella, L.H. Vu, ALABC Project No. AMC-009, Final report, CSIRO Div. Minerals, December 1995–November 1997, Melbourne.
- [3] K. Jana, *The Battery Man* 41 (1999) 28.
- [4] M. Calábek, K. Micka, P. Bača, P. Křivák, V. Šmarda, *J. Power Sources* 67 (1997) 85.
- [5] M. Calábek, K. Micka, P. Bača, P. Křivák, L. Šácha, ALABC Project No. B-001.1, Progress report No. 1, October–December 1997, Technical University Brno, 66209 Brno, Czech Republic, December 1997, p. 27.
- [6] M. Calábek, K. Micka, P. Bača, P. Křivák, L. Šácha, *J. Power Sources* 78 (1999) 94.
- [7] A.F. Hollenkamp, M. Calábek, K.K. Constanti, M.J. Koop, K. McGregor, K. Micka, ALABC Project No. AMC-003, Progress report No. 6, July–September 1994, CSIRO Div. Minerals, Melbourne, 1994.
- [8] M. Calábek, K. Micka, P. Bača, P. Křivák, V. Šmarda, *J. Power Sources* 62 (1996) 161.
- [9] M. Calábek, K. Micka, P. Bača, P. Křivák, L. Šácha, ALABC Project No. AMC-010, Final report, October 1995–September 1997, Technical University Brno, 66209 Brno, Czech Republic, December 1997, p. 84.
- [10] M. Calábek, K. Micka, P. Bača, P. Křivák, V. Šmarda, *J. Power Sources* 64 (1997) 123.
- [11] M. Calábek, K. Micka, P. Bača, P. Křivák, L. Šácha, in: *Proceedings of the Conference of 4th ALABC Members & Contractors*, Vol. 1, Scottsdale, Arizona, April 28–May 1, 1999, p. 9.
- [12] D. Pavlov, E. Bashtavelova, *J. Electrochem. Soc.* 133 (1986) 241.
- [13] E. Bashtavelova, A. Winsel, *J. Power Sources* 46 (1993) 219.
- [14] D. Pavlov, S. Ignatova, *J. Appl. Electrochem.* 17 (1987) 715.